Inversion of Lloyd Mirror Field for Source Track Information

Michael J. Wilmut and N. Ross Chapman

School of Earth and Ocean Sciences, University of Victoria, B C, Canada

ABSTRACT

This paper describes a computationally efficient inversion technique for determining the depth and speed of a sound source that is emitting a set of high signal-to-noise ratio tones. It is assumed that the source is moving at constant heading, speed and depth in shallow water, and passes close by a bottom moored hydrophone. At short ranges, the acoustic field consists of a dominant signal from the direct and surface reflected Lloyd mirror (LM) component, and a series of bottom reflected paths that modulate the LM signal. A computationally efficient propagation model based on the method of images is developed to calculate modelled fields for the inversion. The matched field inversion method for inferring the source depth, speed, and closest point of approach from a single hydrophone is demonstrated using data an experiment carried out in shallow water off the east coast of Canada. The results from the experimental data for the individual hydrophones were combined to give information about the source track. These results are compared with independent measurements of the track geometry that were taken at the time of the experiment.

INTRODUCTION

Matched field processing (MFP) has been successfully used many times to localize an acoustic source in shallow water (Tolstoy, 1993). The idea in MFP is that source parameters can be determined by matching modelled vectors from the acoustic field with the measured data itself. In most reported cases the measured data are from a horizontal or vertical array, with sufficient aperture to allow for the necessary source spatial discrimination. Results for single hydrophone source localization have also been reported (Jesus, 2000), from experiments in which the source range to the hydrophone was a few kilometres. The necessary spatial discrimination was obtained by using a broadband source.

Propagation codes exist for modelling shallow water propagation but they are in general computationally slow. Here a fast and efficient method is described to model short range propagation. The method is used in an MFP application to track a source from experimental data. More precisely it is assumed that a multitone acoustic source, which is moving at constant heading, speed and depth passes close by a bottom moored hydrophone. At short ranges the acoustic field consists of a dominant signal from the direct and surface reflected Lloyd mirror (LM) component, and a series of bottom reflected paths that modulate the LM signal. A computationally efficient propagation model based on the method of images is developed to calculate modelled fields for the inversion. The Theory section contains a brief summary of the method of (LM) images as well as a description of the MFP matching function. Next, a summary of LM-MFP applied to synthetic examples is given. The complicated spatial structure of the acoustic source pressure, which creates the conditions necessary for source depth discrimination, is illustrated. The method is then applied to data from an experiment carried out in shallow water off the east coast of Canada. The source geometry estimates (SGE): source depth, source speed, closest point of approach (CPA) and time of CPA obtained are compared to measurements taken at the time of the experiment. SGEs from individual hydrophones are then combined to give information about the source track. A summary section includes a discussion of avenues of future research.
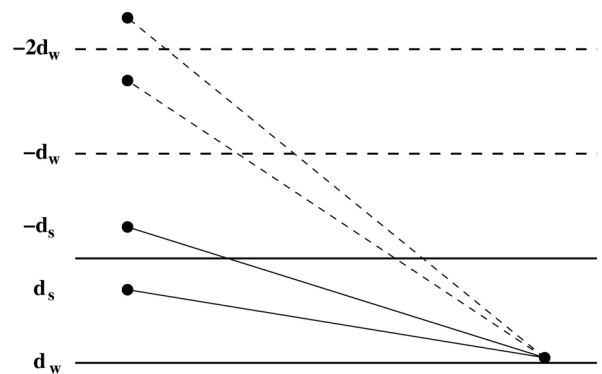

Figure1. Multipath components from the source and its images for the first signal path to the bottom receiver. The water depth is d_w and the source depth is d_s.

THEORY

Lloyd Mirror Propagation Model

The objective is to develop a simple propagation model that describes the spatial structure of the acoustic field at short ranges, less than a few water depths. We formulate the field in the shallow water channel using the method of images (Brekhovskikh, 1991). The field is given by the coherent sum of the contributions from the source and its images. Each image generates a component of the multipath signal. Figure 1 shows the real source and the image sources for the first four signal paths to the bottom receiver: the direct path, and the sea surface reflection, and the (two) first-order bottom reflections. For the special case of a receiver on the sea floor, there is only one set of images, reflected through the sea surface. The multipath components of the field can be organized conveniently into pairs, with one member of each pair having an additional sea surface reflection. The direct path and sea surface reflection pair is a simple example; all subsequent orders of bottom reflections can be organized in the same manner. All bottom reflected components have at least one sea surface interaction for this geometry.

For the direct path component at the bottom receiver, the pressure at frequency f is given by

$$p_d = \frac{\exp ikR}{R}(1+V) \, ,$$

1

where V is the complex reflection coefficient at the sea floor, R is the distance from the source to the receiver, and $k = 2\pi f/c_w$ with c_w the speed of sound in water. The reflection coefficient is a function of the densities and sound speeds in water and in the sea bottom (Brekhovskikh, 1991). Critical angle reflections are modelled within the limitations of the ray approximation. The term $1+V$ accounts for the pressure at the seafloor, and must be included for each component of the signal at the bottom receiver. Expressions of the same form can be generated for the other components of the field by multiplying by -1 whenever the image ray intersects the sea surface images, and by V whenever the image ray intersects the ocean bottom images.

The components of the field can be separated into two groups, in terms of the direction of the ray path at the source. The first group is effectively a down-going field. These components have a vertical position coordinate of the source or image identified by $((2n+1)d_w − d_s)$, where n = 0,1,... Here d_w is the water depth and d_s is the source depth. The terms are summed as

$$p_- = \sum_{j=0} (-1)^j (V_-)^j \frac{\exp(ikR_-)}{R_-}(1+V_-) \cdot$$

2

For the down-going field (denoted in Equation 2 by the subscript (−)), the range is given by $R_- = \sqrt{((2n+1) d_w - d_s)^2 + r^2)}$, where r is the horizontal distance from source to receiver. The second group is an up-going field (denoted by the subscript (+)), and its components are identified by a vertical position coordinate of the form $((2n+1)d_w + d_s)$, where n = 0,1,.. The terms are summed as

$$p_+ = \sum_{j=0} (-1)^{j+1} (V_+)^j \frac{\exp(ikR_+)}{R_+}(1+V_+)$$

3

and the range is given by $R_- = \sqrt{((2n+1)d_w + d_s)^2 + r^2)}$. The total field is then $p_T = p_- + p_+$. The expressions for the up- and down-going fields can be modified to include scattering at a rough sea surface. Similarly, reflection from an elastic sea bottom can be included by replacing the appropriate reflection coefficient for one that accounts for shear waves.

At short ranges (less than a few water depths) the pressure field calculated with the image method propagation model agreed well with pressures calculated using both the normal mode and parabolic equation methods for cases that included critical angle reflections (Chapman, 2003). Performance limitations for an inhomogeneous sound speed profile in the water were also investigated previously (Chapman, 2003).

We assume for applications in shallow water that the environment is approximated by a Pekeris waveguide: constant sound speed in the water c_w, fixed water depth d_w, and basement sound speed c_b and basement density ρ, respectively. We also note that in practical applications the summations in Equations 2 and 3 can be limited to two or three terms.

Source geometry estimates

Assume a multitone source is moving at constant bearing, speed, s, and depth, d_s, in a shallow water environment. When the source passes close to a sea floor hydrophone, its pressure recorded at the hydrophone will be modelled pri-

marily as LM propagation. The closest point of approach to the hydrophone occurs at time t_{cpa} and at a distance of R_{cpa}. The objective is to determine estimates and uncertainties of these four source parameters, called the source geometry estimates (SGEs). The measured and modelled amplitude data at a specific frequency f and time i are denoted $d_{i,f}$ and $d_{i,f}(m)$, respectively, where i = 1,2,.. ,n_t and f = 1,2,..n_f. The quantity n_t is the number of contiguous time intervals (snapshots) that have been Fourier transformed to obtain the measured amplitude data. The model m is made up of the four geoacoustic parameters for the Pekeris waveguide and the four SGEs. Assuming the data errors are zero mean Gaussian distributed random variables uncorrelated over time and frequency with common standard deviation σ_f at each frequency, the likelihood function is given by

$$L(m,\sigma) = \prod_{f=1}^{n_f} \frac{1}{\left[\sqrt{2\pi} \, \sigma_f\right]^{n_f}} \exp(-\sum_{i=1}^{n_t}\left[d_{i,f} - (A_f + B_f d_{i,f}(m))\right]^2 / 2\sigma_f^2)$$

4

where A_f and B_f are scaling parameters since $d_{i,f}$ is measured data and $d_{i,f}(m)$ is modelled data. Setting $\partial L/\partial A_f = 0$ and $\partial L/\partial B_f = 0$, solving for A_f and B_f, and substituting the result into Equation 4 gives

$$L(m,\sigma) = \prod_{f=1}^{n_f} \frac{1}{\left[\sqrt{2\pi} \, \sigma_f\right]^{n_f}} \exp\left(-\left[\sum_{i=1}^{n_t} d_{i,f}^2\right] E_f(m)/2\sigma_f^2\right)$$

5

where

$$E_f(m) = 1 - \frac{(\sum_{i=1}^{n_t} \widetilde{d}_{i,f} \widetilde{d}_{i,f}(m))^2}{\sum_{i=1}^{n_t} \widetilde{d}_{i,f}^2 \sum_{i=1}^{n_t} \widetilde{d}_{i,f}^2(m)}$$

6

Here $\widetilde{d}_{i,f}$ and $\widetilde{d}_{i,f}(m)$ are $d_{i,f}$ and $d_{i,f}(m)$, respectively, with their time averages subtracted. To estimate the variances in Equation 5, maximize L by setting $\partial L/\partial \sigma_f = 0$ which gives

$$\sigma_f^2 = \exp(-\left[\sum_{i=1}^{n_t} d_{i,f}^2\right] E_f(m)/n_t)$$

7

Finally, substituting the estimate for σ_f into Equation 5 yields

$$L(m) \propto \frac{1}{\prod_{f=1}^{n_f} E_f(m)^{n_t/2}} \cdot$$

8

This is the implicit form of the likelihood function (Dosso and Wilmut, 2006). The MAP (maximum *a posteriori*) estimates of *m* are those that maximize L(m). In practice we minimize an expression that has the same extrema, E(m), where

$$E(m) = \left[\prod_{f=1}^{n_f} E_f(m)\right]^{1/n_f} \cdot$$

9

The minimization is carried out using the optimizer Adaptive Simplex Simulated Annealing (ASSA) (Dosso, 2001) to obtain the MAP estimates. ASSA is an easy to use hybrid optimization algorithm which combines a random global search method, simulated annealing, and a local gradient-based search method, downhill simplex. It is an effective and efficient method to determine the global minimum of a multidimensional function which has many local minima, strong correlated parameters, and a wide range of parameter sensitivities.

APPLICATION TO SYNTHETIC DATA

A number of synthetic data sets were generated using a Pekeris waveguide (water depth 100 m, water sound speed 1485 m/s, sediment sound speed 1600 m/s, and density 1.8 g/cm^3) and various source geometries. Zero-mean, Gaussian noise was added to the signal to yield various signal-to-noise ratios (SNR). The source was assumed to consist of six evenly spaced tones with frequencies between 50 and 150 Hz. This data was then inverted using ASSA. It was found that good source depth and speed estimates were obtained for SNR as low as 47 dB, source depths between 4 and 80 m, and CPAs between 5 and 125 m, whenever the objective function minimum (Equation 9) was less than or equal to 0.20. The CPA was not as well estimated. Lower SNR's were required for good source depth estimation when more frequencies were used and/or the CPA was small.

The ability to discriminate source depth can be explained by the LM beam structure. The number of beams, M, for a source that passes the hydrophone at close range is given by M = 2 int(d_s/λ + 0.5), where λ is the acoustic wavelength (Jensen, 1994).

Figure 2 displays these beams for a frequency of 100 Hz and depths 5, 10, .., 80 m. The increasing number of beams as depth increases is easily seen as well as the fact that the beam structure changes rapidly over depth. The beam structure also changes as a function of CPA, especially for deeper sources. The source speed also causes a noticeable change in the beam structure.

In summary the synthetic study showed that good SGEs are obtained under a variety of "real world" scenarios. These results can be explained by the complex acoustic propagation structure.
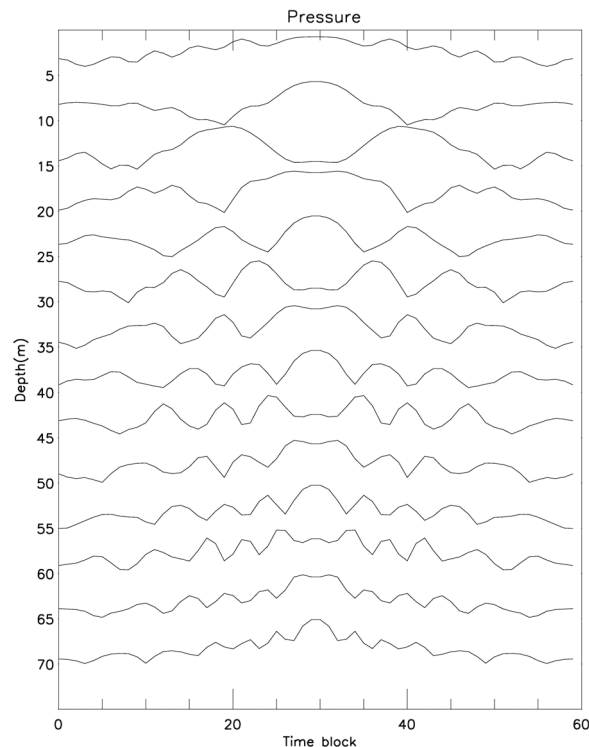

Figure 2. LM pressure field versus time block for various source depths.

APPLICATION TO EXPERIMENTAL DATA

Field Test STM01

A field test was conducted by Defence R&D Canada in July 2004 in St. Margrets Bay, a shallow water area off the southern coast of Nova Scotia, Canada. A rapidly deployable 80 m long array with 24 working hydrophones was laid out in an approximately linear configuration. In order to test the LM-MFP concept a projector continuously generating tones at 72, 87, 93 and 111 Hz was towed in a straight line at a speed of about 1 m/s and depth 20 m close by the array on two occasions. The time series were Fourier transformed in eight second time blocks. The total pressure of the above four frequencies as a function of time block is given in Figure 3 for hydrophone 27. The approximate CPA time block of 130, where the pressure is the maximum, is well defined. The left limit for the measured data is the first time block less than 130 such that the total pressure is less than or equal to 0.3 times the maximum pressure. The right hand limit is the first time block greater than 130 where the same condition holds. The resulting measured data is the solid curves of Figure 4. The average pressure over the processing time at the narrowband signal frequencies divided by the average pressure at its neighbouring non-signal frequencies ranged from 15-23 dB.
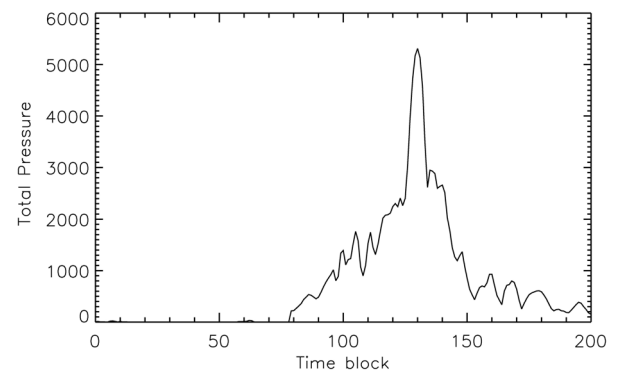

Figure 3. Total pressure of the four source frequencies as a function of time block for hydrophone 27.
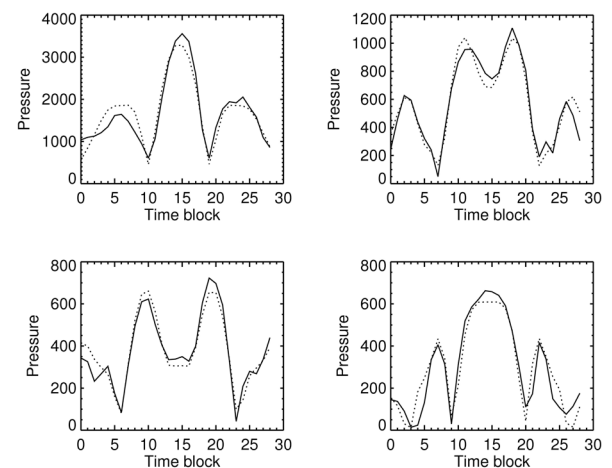

Figure 4. Measured (solid line) pressure versus time block for 72 Hz (upper left), 87 Hz (upper right), 93 Hz (lower left0 and 111 Hz (lower right). The dotted line is the modelled pressure.

Source Geometry Estimates

The measured hydrophone 27 data was inverted using ASSA. The minimum value of the objective function for the MAP estimate was 0.077. A plot of the modelled data is the dotted curve of Figure 4. Not surprisingly, given the value of 0.077,

the fit is very good. A plot of accepted parameter values versus objective function is displayed in Figure 5. The search bounds for the eight parameters can also be seen in the figure. They were based on measurements taken during the experiment. Figure 6 is a plot of the downward refracting sound speed profile (SSP) taken during the experiment. It is interesting to note that while this SSP differs from the modelled uniform SSP the measured data was still fit very well. The distribution of points about the minimum value in Figure 5 provides a useful measure of the sensitivity of the parameter and a qualitative indication (for parameters associated with a low value of the objective function) of which parameters have been well estimated. A sensitive parameter is one for which a small change in the parameter near the minimum results in a large change in the value of the objective function. For this case we observe that source depth, speed and time of CPA are sensitive parameters, CPA and water depth are less sensitive and the geoacoustic parameters were insensitive. These sensitivity results were consistent with those observed during the synthetic study. The SGE's for a selected set of hydrophones, including hydrophone 27, are given in Table 1, where the CPA time of hydrophone 27 was arbitrarily set to 0 s.

Table 1. SGEs for selected hydrophones.

h/p	t_cpa(s)	R_cpa(m)	d_s(m)	s(m/s)
8	46.6	19.8	22	0.95
14	33.2	14.4	23.2	0.96
22	13.2	3.0	23.8	1.0
24	3.5	3.1	24	1.03
27	0.0	2.3	24.3	1.06

The estimated source depth values in Table 1 are consistent (22.0-24.3 m) and agree with the reported estimate of 20 m from the experiment. As well the source speeds are consistent (0.95-1.06 m/s) and agree with measurement of an average speed of 1 m/s taken during the field trial. In fact the source depth and speed estimates were consistent for data from all the 24 working hydrophones.
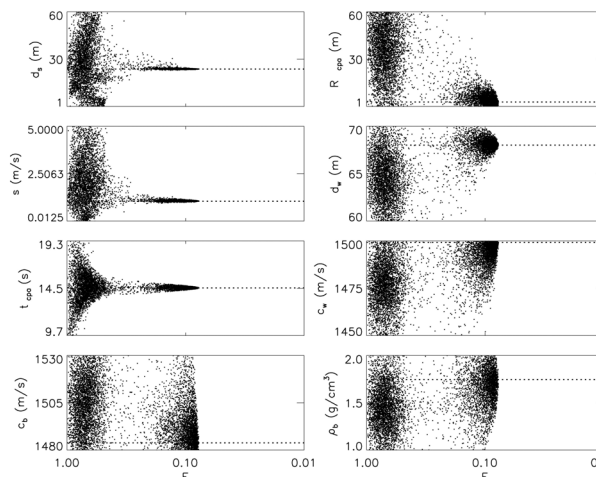

Figure 5. ASSA accept parameter values versus objective function for the eight geoacoustic and source parameters. Dotted lines are the MAP estimates.

Source Track Information

The SGEs obtained from the individual hydrophones were then combined to provide information about the source track. Figure 7 plots the (x, y) coordinates of the 24 working hydrophones as diamonds. The circles about the hydrophones
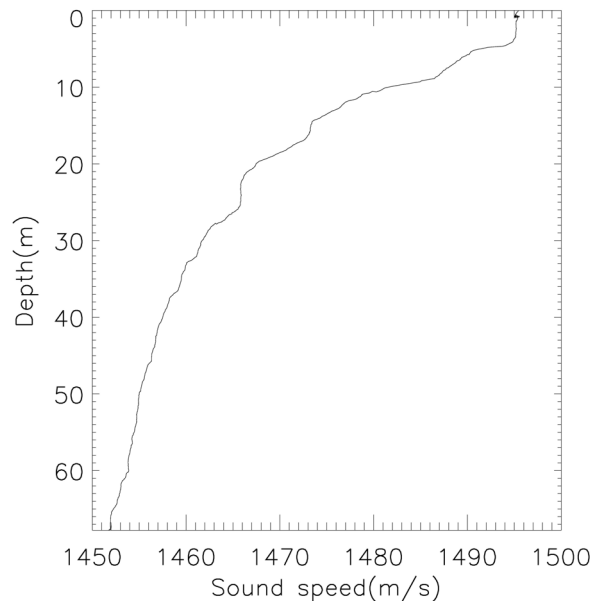

Figure 6. Measured Sound speed profile.

listed in Table1 represent the CPA estimates for the hydrophone with the CPA estimated times noted as well. In theory a source travelling linearly at constant speed (here approximately 1 m/s the average of the five speed estimates of Table 1) would be a line on the figure tangential to the circles. Distances along the line where the line touches the circles should correspond to the differences between the CPA times multiplied by the average speed. The direction of the track would be associated with increasing CPA times. From the figure and observations above it is most likely that the source is travelling in a northwest direction passing close by hydrophone 27 about time 0 and crossing the array between hydrophone 14 and hydrophone 22. From GPS measurements taken during the experiment this was indeed the source track direction.

The LM propagation code is very simple to code and is very fast to execute. The per hydrophone inversions only took about one and a half minutes to run in IDL on a 2.6 GHz CPU. This implies that information about the source track can be obtained in almost "real time".

DISCUSSION

LM-MFP has been successfully shown to estimate the track of a high SNR multi-tone acoustic source travelling at constant heading, speed and depth in shallow water close by a set of bottom moored hydrophones. The track can be estimated in almost real time. The ability to track is due, in large part, to the high spatial discrimination provided by the LM beam structure. The method worked in spite of the fact that the measured sound speed profile differs from the uniform sound speed profile assumed in the LM propagation code.

The approximately linear, evenly and closely spaced hydrophone array described above was used to show that the LM concept can be used to efficiently model short range propagation in shallow water and hence perform source detection. A possible practical implementation would be to place the array elements as above but with a spacing of about half a water depth. Such an array would be able to estimate the track of a high SNR source as it moves through this barrier. An open question for future study is an estimate of the lowest SNR required to obtain good SGEs and hence a good track estimate.
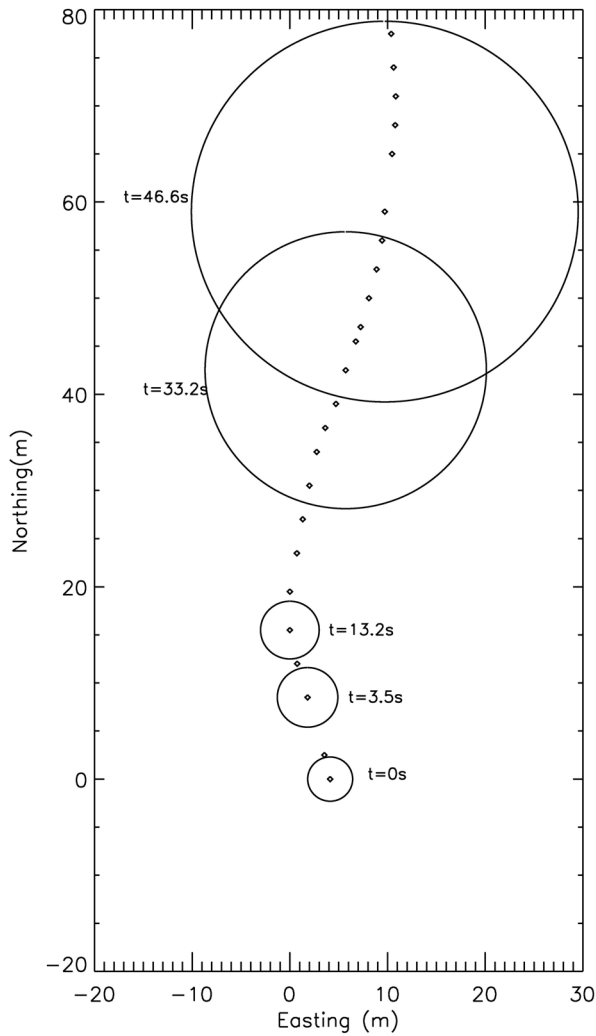
Figure 7. Deployed hydrophones (diamonds) with the northernmost hydrophone being number 2. Estimated CPA and time of CPA for selected hydrophones.

REFERENCES

Brekhovskikh, L M, and Lysanov, Y P 1991, *Fundamentals of Ocean Acoustics*, 2nd edn, Springer-Verlag, New York.

Chapman, N R, Heard, G J, and Chapman, D M F 2003, 'Lloyd's mirror matched field processing in shallow water', *10th International Congress on Sound and Vibration*, Stockholm, Sweden.

Dosso, S E, Wilmut, M J, and Lapinski, A L, 2001, 'An adaptive hybrid algorithm for geoacoustic inversion', *IEEE Journal of Oceanic Engineering*, vol.26, pp. 324-336.

Dosso, S.E., and Wilmut, M.J., 2006, 'Data uncertainty estimation in matched field geoacoustic inversion', *IEEE Journal of Oceanic Engineering*, in press.

Jensen, F B et al 1994, *Computational Ocean Acoustics*, American Institute of Physics Press, New York.

Jesus, S M, Porter, M B, Stephan, Y, Demoulin, X, Rodriguez, O C, and Coelho, E M M F 2000, 'Single Hydrophone Source Localization', *IEEE Journal of Oceanic Engineering*, vol.25, pp. 337-346.

Tolstoy, A 1993, Matched Field Processing for Underwater Acoustics, World Scientific Press, Singapore.